Nuclear Materials Authority
P.O.Box 530 Maadi, Cairo, Egypt

ISSN 2314-5609
Nuclear Sciences Scientific Journal
8, 203- 211
2019
http://www.ssnma.com

WELL LOGGING ANALYSIS FOR ESTIMATING POROSITY IN FRACTURED BASEMENT RESERVOIRS

MAHMOUD E. ABDELRAZIK
Nuclear Materials Authority,P.O. Box – 530 Maadi, Cairo, Egypt

ABSTRACT

Low porosity fractured reservoirs have been successfully described, using a combination of high resolution geometrical information from borehole images, together with deeper penetrating log evaluation methods. Borehole images from acoustic or electrical scanning tools provide statistics of the fracture distribution, first order estimates of fracture opening and porosity, and a basis for geological inferences. Their drawback is that, in this environment, the events on the images bear a strong overprint of the drilling process. Deeper penetrating, but lower resolution techniques, such as Stoneley wave reflectance and deep resistivity log inversion are used to distinguish the deep and permeable fractures that may contribute to flow. By making some assumptions about the nature of porosity in basement reservoirs, we develop a new method to estimate the porosity and the fraction of this secondary porosity is developed due to fractures. This method makes the use of the Kuster-Toksoz acoustic scattering model and requires low frequency measurements of compressional and shear velocities.

INTRODUCTION

In their study on the basement reservoirs of the continental shelf off the southern coast of Vietnam, Areshev et al., (1992) found that the effective porosity was due to three components: Fractures of tectonic origin, vugs (cavernous porosity) of hydrothermal origin and pores caused by near-surface weathering. The porosity distribution is thus very irregular. High porosities tend to be concentrated in the breccias associated with large faults, however high porosity intervals are often widely separated by low porosity and permeability intervals. In the White Tiger field, the average core porosity in the deeper basement sections was less than three percent and divided almost equally into fractures. Evaluation of reserves from well logs in such conditions is not straightforward. The well samples in which the logs are acquired are localized only in a very small part of an irregularly distributed fracture-pore network, and it is by no means obvious, whether such a sampling is statistically significant for reserves estimation. At such low overall porosities, the error in estimating porosity using conventional porosity logging techniques is close to the measurement itself. Moreover, the variations in rock properties, such as density, hydrogen index and borehole damage, which affect the shallow reading devices, can be mis-interpreted as changes in porosity. For this reason, the quantitative estimation of subsurface fracture porosity and fracture permeability has been considered to be highly variable and mostly inaccurate (Nelson,1982). Acoustic velocities, derived from array-sonic devices, have proven to be less sensitive to borehole damage, than the density and neutron devices; and in the non-fractured granitic rocks, the velocity tends to the high relatively constant values. Keys

(1979) reported the average values of the compressional slowness of 50–52 microsec/ft over thousands of feet of granitic intrusive rocks. This invariability of the host rock properties, together with the sensitivity of acoustic properties to fracturing, yield a number of different techniques to detect fractures. Compressional and shear wave attenuations have been used for fracture indication [(Morris et al., 1964), (Koerperich, 1978) and (Cheung, 1984)] and it was discovered that, the attenuations of both compressional and shear waves are varied with the fracture angle. A further observation was that, whereas the ratio of compressional to shear waves velocity, Vp/Vs, is constant in the non-fractured rocks, it increases whenever there are more fractures. Logging tools review recent work on the acoustic wave forms has focused on the tube or Stoneley wave, [(Poeter, 1987), (Paillet, 1991a, b) and (Hornby et al., 1989)]. For single large fractures in a rigid formation, the width or aperture of the fracture (denoted by the Greek letter e) can be determined from the amplitude of the reflected Stoneley wave. In boreholes without significant mud-cake, continuously varying values of permeability can be determined from the dispersion and attenuation of the Stoneley wave [(Chang et al., 1988), (Norris, 1989) and (Winkler et al., 1989)].

Deep resistivity logging devices, in particular the Dual Laterolog (DLL†), are also extensively used for fracture evaluation. Boyeldieu and Winchester, Boyeldieu and Winchester, (1982) derived an estimate of the fracture porosity, Ø, from the difference in conductivities between the shallow and deep laterologs:

$$DC = C_{LLs} - C_{LLd} = m_{frac} C_m, \qquad (1)$$

where C_{LLs} and C_{LLd} are the conductivities in S/m measured by the deep and shallow laterologsrespectively, C_m is the conductivity in S/m of the mud (which is assumed to have invaded the fractures) and m_{frac} is the Archie, formation factor exponent of the fracture network (usually around 1.4).

Sibbit and Faivre (1985) showed later that, the quantity DC is proportional to the fracture aperture e for long vertical fractures and proposed the following formula:

$$DC = 4.10^{-7}.e.\ C_m, \qquad (2)$$

where; the fracture aperture (e) is in microns. For single horizontal fractures, a somewhat different formula was proposed:

$$C_{LLd} - C_b = 12\ (10^{-8}) e\ .\ C_m\ , \qquad (3)$$

where C_b is the conductivity of the non-fractured host rock.

Since many of the fractures encountered in the subsurface are high-angled or close to vertical, there is a tendency to use Eq. 2 to estimate the fracture aperture. This is not always the correct way, as the extent of the fracture along the borehole needs to be taken into account, and very often Eq.(3) is more appropriate. Faivre (1993) in extending this work to the Azimuthal Resistivity Imager (ARI†), describes more fully the effect of fracture dip and proposes:

$$e = \frac{a.AA\,C_b}{C_b^{\,c}\,.\,C_m^{\,1-c}} \qquad (4)$$

where; AAC is the area of the conductive anomaly in conductivity-thickness units (S/m.m) of the conductive anomaly due to a fracture, and a, b and c are constants (b»1, and c is very small). Equation of this form applies to the deep, shallow and high-resolution deep laterologs.

Equation (4) is very similar to the form derived by Luthi and Souhaité (1990) for the Formation Micro-Scanner tool or Formation Micro-Imager tool (FMS†,FMI†). Although the high-resolution information from this tool comes from close to the borehole, the measured current is sent deep into the formation permitting the tool to be compared and calibrated with the shallow laterolog resistivity. In addition to the quantitative estimates of fracture aperture, the geometry of fractures intersecting the borehole can be determined. Statistics on the distribution of borehole intersecting fractures are best gathered on the image processing work station of Cheung and Heliot (1990). The geometrical distribution of

fractures together with the fracture apertures information enable us to estimate the fracture porosity provided that, the fractures are sufficiently widely spaced and resolvable enough by the measuring device. The acoustic imaging tools can also be used to quantify the fracture geometry, but they are very shallow reading devices and are strongly influenced by the borehole conditions. Both the amplitude and transit-time images and recorded by borehole televiewers and other acoustic scanning devices, are surface images and can be considered the result of reflection at or close to the boreholewall. This has both disadvantages and advantages. The images bear a strong imprint of the drilling process, such that the natural fractures may be obscured by the drilling induced well-bore damage. An advantage is that, the state of operating stress-can be inferred from the analysis of induced fractures, break-† Mark of Schlumberger outs, and shear displacements as shown by Addis (1993). In addition, the acoustic scanning devices have 360° coverage.

RECOMMENDED LOGGING SUITES

High resolution formation images are necessary to determine the fracture geometry and to resolve small fractures. Electrical scanning devices, such as the FMI "see" deeper through the formation than the acoustic scanning devices, which return back by a surface image. A borehole surface image is useful for determining the state of in-situ stress, but is somewhat more difficult to interpret it in terms of formation properties. Whether a fracture with an electrical device depends on the magnitude of the conductive anomaly. A good rule of thumb is that, the product of the fracture width and the mud conductivity should be roughly an order of magnitude bigger than the product of the measure-current beam width and the conductivity of the host medium as exhibited through the following equation:

$$\varepsilon \,.\, C_m \approx 10.(\text{beam} - \text{width}).\, C_b \qquad (5)$$

where; beam-width is 0.5 cm for the FMI, 15cm for the high resolution laterolog of the ARI and 90cm for a conventional deep or shallow laterolog.

Both the laterolog data and electrical images are required for quantitative work. The shallow laterolog is used to calibrate the FMI images in terms of resistivity, and the deep laterolog provides a measurement of the aperture of deeply invaded fractures. The fracture distribution is directly measured on the FMI image. Permeability is best estimated from the Stoneley wave, as described in the papers discussed above, or measured directly. Individual fracture sets can be tested between straddle packers with a wireline formation tester. Low frequency reflected Stoneley waves, probe deep into the formation, are sensitive to the aperture of open fractures and are insensitive to induce fractures. Estimates of fracture aperture are directly comparable to those from deep electrical devices as shown by Hornby and Luthi (1992). Low frequency compressional and shear velocities can also be used to make an estimate of porosity as described later. An advantage of this technique is that, it may be extended to the seismic frequency, and the porosity within the basement may be mapped, whenever there is sufficiently good velocity data.

FRACTURE ESTIMATES BY THE DUAL LATEROLOG TOOL

Figure (1) shows the response of the Dual Laterolog tool; as it approaches a horizontal fracture of 50 micronswidth, in a borehole filled with mud of 0.1 Ohm.m resistivity. The non-fractured formation resistivity is 10,000 Ohm.m. The anomaly on the log, due to the fracture, is a sharp decrease in resistivity, approximately 90 cm wide (current beam-width of the dual laterolog). For fractures of small extent along the borehole, i.e. shallow-angle, the resistivity in front of the fracture is given by Eq.(3). Alternatively, the area under the conductivity curve AAC (can be shown in Fig. 2) and Eq. (4) can be used.

Figure (3) shows a short vertical fracture of 500 microns width, with the same mud and formation resistivity. The appearance of the anomaly is similar to that of Fig.(1). Note that, there is no separation between the shallow and deep laterologs and as a consequence, Eqs. (1&2) would under estimate the fracture porosity and opening, while Eq.(4) gives good answers. The fracture on Fig.(3), is one meter long and the width of the anomaly on the log is approximately 1.9m. Note also the appearance of resistivity horns at the boundaries of the fractures. A long vertical fracture was modeled to generate Fig.(4). At the center of the fracture, the deep and shallow laterologs separate. Either Eq.(3) or Fig.(5) may be used to estimate the fracture opening.

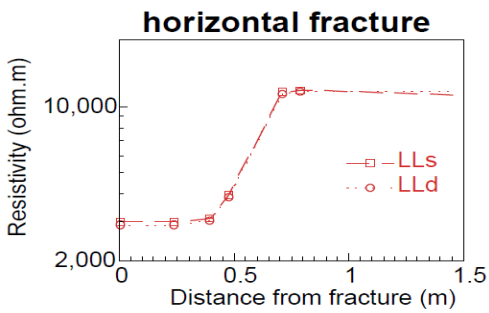

Fig.1:Modeled Dual-Laterolog Tool Response of a 50 Micron Horizontal Fracture filled with 0.1 Ohm.m mud in a 10,000 Ohm.m formation. Only half the fracture is shown, as the log response is symmetrical about the fracture position

ESTIMATING FRACTURE POROSITY FROM THE COMPRESSIONAL AND SHEAR VELOCITIEs

Brie et al. (1985) used an acoustic scattering model to understand the variation of compressional and shear velocities in carbonates with oolitic porosity. Their method is appropriate also for small concentrations of fractured porosity in igneous and metamorphic rocks. Since basement rocks are well-cemented, the primary effect on acoustic velocity is due to pore shape and concentration. Pore shape can be characterizedby the pore aspect ratio. Fractures are modeled as ellipsoids (disks), whose aspect ratio is more less than 1.

The aspect ratio can be approximated by the fracture aperture divided by the fracture length. In the basement rocks, the isolated fractures will have very small aspect ratios in the range, 0.001–0.01 say, whereas for the fractures in breccias, the ratio is closer to 0.1. To simplify the evaluation, it can be assumed that, the sonic tool responds to porosity in

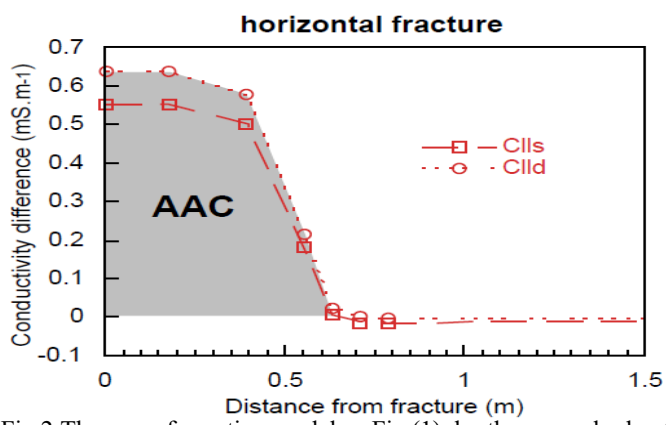

Fig.2:The same formation model as Fig.(1), by the anomaly due to a horizontal fracture is viewed in conductivity units

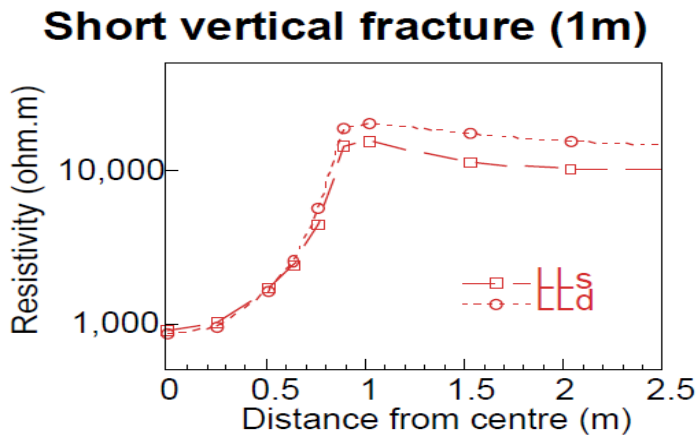

Fig.3:Short vertical fracture of 1 metre long and 500 micronsaperture. Compare with the horizontal fracture response of Fig.(1)

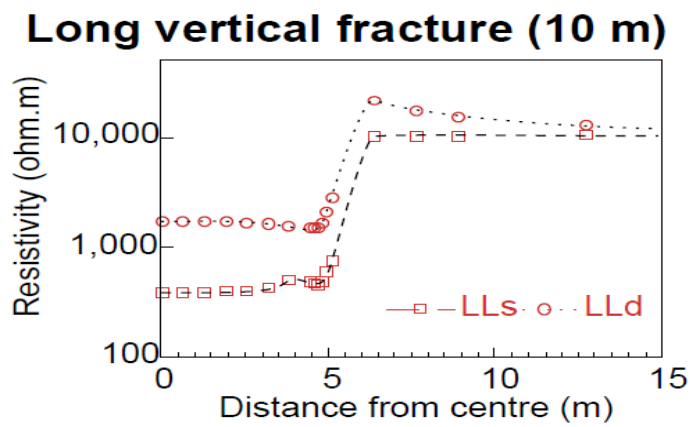

Fig.4:Long vertical fracture 10 metre long, aperture 500 microns. Note the resistivity horns at the fracture boundaries

the breccias (inter-particle porosity) much the same way as it does to the inter-granular porosity in a more conventional reservoir. Again following Brie et. al., (1985), Berryman, (1980) derivation was used for the acoustic scattering from ellipsoidal inclusions in an elastic medium. At sonic logging frequencies (<10 kHz), the wavelength is much greater than the pore size and the average scattering properties of the different types of fractures in the formation we can be considered. At seismic frequencies, the wavelength is always greater than theaverage fracture spacing. We model first the host rock, assuming that, for non-fractured and interparticle porosity (such as that found in the breccias), the compressional slowness follows Wyllie time average formula:

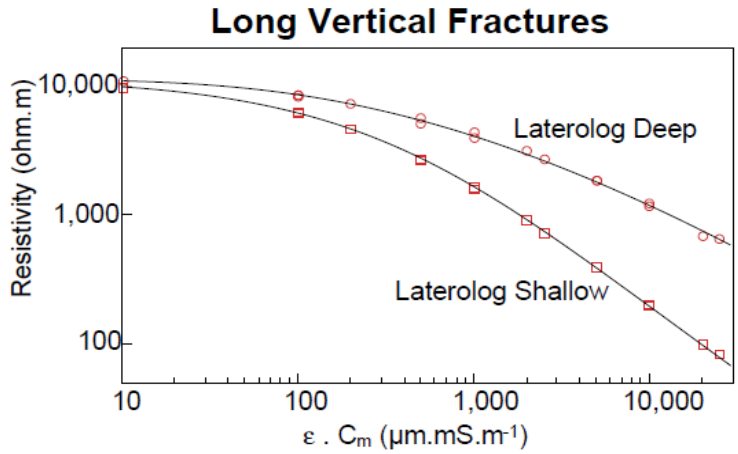

Fig.5:Chart for estimating the fracture opening for long vertical fractures

$$1 / Vp = \Delta tb = (1-\phi)\Delta tb + \phi \Delta t f \quad (6)$$

where;ϕ is the non-fractured porosity, Δtf is the fluid slowness and Δtb is the rock slowness.

We assume also that, Pickett's relationship applies for the non-fractured rock:

$$\frac{v_p}{v_s} = \frac{\Delta t_s}{\Delta t_p} = \text{constant.} \quad (7)$$

The density follows the relationship:

$$\rho_b = \phi \rho_f + (1-\phi)\rho_m. \quad (8)$$

where: ρ_f is the fluid density and ρb is the rock density.

Using Eqs. (6,7 & 8), we model the variation of acoustic velocities, V_p and V_s, and density ρ with porosity. The bulk and shear moduli of the rock are given by Eqs. (9 and 10) as shown as follows:

$$K_b = \rho v_p^2 \left(1 - \frac{4v_s^2}{3v_p^2}\right), \quad (9)$$

$$G_b = \rho v_s^2. \quad (10)$$

where: K_b is the bulk modulus and G_b is the shear modulus.

Introducing a fraction fi of ellipsoidal inclusions (fractures) into the rock changes, the porosity to f(1-fi)+fi and the elastic constants. The resulting effect on the compressional and shear slownesses is plotted on Figs.(6&7). The black circles are spaced at 1% porosity intervals and represent increasing non-fractured or inter-particle porosity.

The lines joining these points represent different specific fractions of the porosity. The aspect ratio is the ratio of the minor to the major axes of the fracture planes. By looking at the interpreted FMI results (mean fracture aperture divided by mean fracture spacing), we chose a ratio of α =0.005 was chosen. This implies that, the average fracture spacing is 200 times larger than the fracture opening (i.e. 10 micron fractures will be spaced every 20 cm. or so). The effect of changing the aspect ratio is also shown for two additional cases α =0.001 and α =0.01. The rock properties used on Figs. (6 &7) are the compressional slowness of 51 microsec/ft and the slowness ratio of 1.7.

These can be compared with a cross plot from a well (Fig.8). The data on Fig.(8), fit the model of Fig.(7), fairly well and show quite

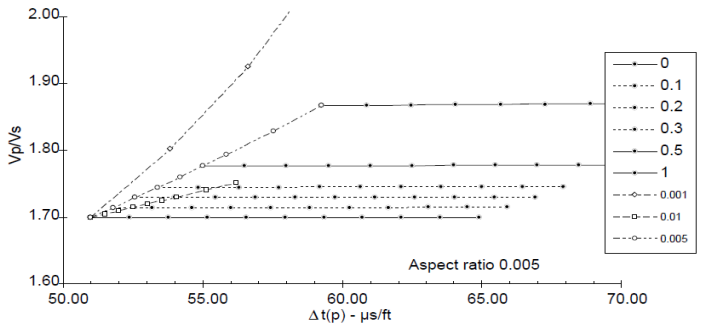

Fig.6:Vp/Vs ratio increases with the fracture porosity for a given fracture aspect ratio

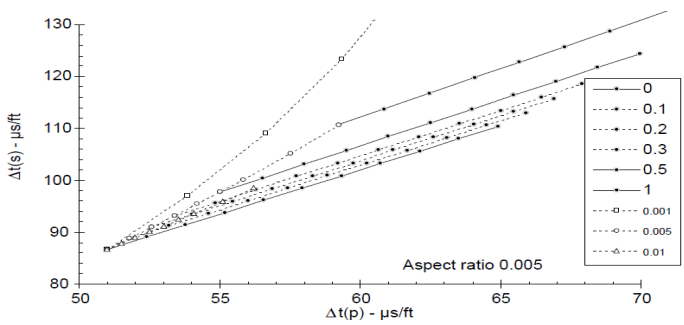

Fig.7:Shear and compressional slowness, as functions of conventional or inter-particle porosity and fractured porosity, as derived from an acoustic scattering model (Kuster and Toksoz, 1974)

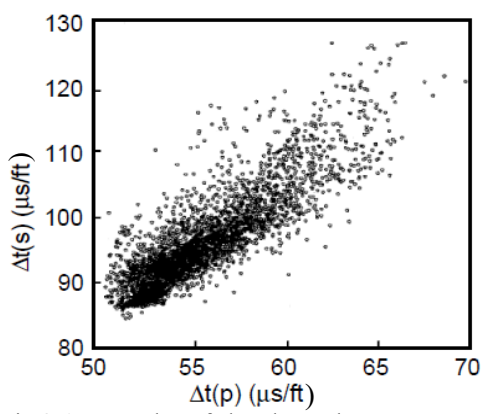

Fig.8:Across plot of the shear slowness versus compressional slowness over a fractured basement interval.The small aspect ratio fractures are concentrated at low porosities. (c.f. Fig. 7)

clearly that, the conventional (Wyllie, Pickett, etc...) sonic models would not fit. In particular, Pickettmodel predicts that, the Vp/Vs ratio should be more or less constant, whereas the model predicts that, the shear slowness increases much more rapidly than the compressional slowness in the fractured intervals. This is what we observe in the field examples. The data fall to the left of the zero porosity trends being due to the fractures with very high aspect ratio, where the shear cannot be supported.

In practice, we measure the Vp and Vs was measured in low porosity intervals and choose an appropriate value of the aspect ratio, a. From the measured values of the com-

pressional and shear slowness in a fractured interval, we derive both the conventional and fractured porosities may be derived.

CONCLUSIONS

Low-frequency acoustic waveform logs provide a robust mean to evaluate the fractures in basement reservoirs. Reducing the frequency reduces the sensitivity of the logs toborehole conditions and averages the formation properties. In addition to the well-known Stoneley wave techniques for deriving fracture aperture, the compressional and shear slownesses may be used to estimate both the conventional and fracture porosity. This technique assumes that, in basement rocks the pore shape controls the compressional and shear slownesses and that, one or two typical pore aspect ratios can be derived by other means.

A typical fractured aspect ratio is the ratio between the fracture opening and fracture spacing, both of which may be estimated from the electrical borehole scans.

REFERENCES

Addis, A., 1993. The Quest for Borehole Stability in the Cusiana Field, Colombia. Schlumberger Oilfield Review, Elsevier Science Publishing Company, Amsterdam, 33-43.

Areshev, E.G.; Tran Le Dong; Thuong San, Ngo, and Shnip, O.A., 1992. Reservoirs in fractured basement, offshore Southern Vietnam. J. Petrol. Geol., 451-464.

Berryman, J.G., 1980. Long-Wavelength Propagation in Composite Elastic Media, Part I: Spherical Inclusions, Part II: Ellipsoidal Inclusions. J. Acoustical Soc. America, 68 (6).

Boyeldieu, C., and Winchester, A., 1982. Use of the Dual Laterolog for the evaluation of Fracture Porosity in Hard Carbonate Formations. The Offshore South East Asia Conf., Singapore.

Brie, A.; Johnston, D.L., and Nurmi, R.D., 1985. Effect of Sperical Pores on Sonic and Resistivity Measurements. The 26th Annual Logging Symposium of the SPWLA, Dallas, USA.

Chang, S.K.; Liu, H.-L., and Johnson, D.L., 1988. Low-frequency tube waves in permeable rocks. Geophysics, 53, 519-527.

Cheung, P.S.Y., and Heliot, D., 1990. Workstation-Based Fracture Evaluation Using Borehole Images and Wireline Logs. The 65th Annual Conf. Soc. Petroleum Engineers, New Orleans, SPE 20573.

Cheung, P.S.Y., 1984. Fracture Detection using the Sonic Tool. The 9th Annual Logging Symposium of the S.A.I.D, Paris.

Faivre, O., 1993. Fracture Evaluation from Quantitative Azimuthal Resistivities. The 68th Annual Conf. Soc. Petroleum Engineers, Houston, SPE 26434.

Hornby, B.E., and Luthi, S.M., 1992. An Integrated Interpretation of Fracture Apertures Computed from Electrical Borehole Scans and Reflected Stoneley waves. In: Geological Applications of Wireline Logs II(Hurst, A., Griffiths, C.M., Worthington, P.F.,Eds.). Geological Society Special Publication, 65, 185-198.

Hornby, B.E.; Johnson, D.L.; Winkler, K.W., and Plumb, R.A., 1989. Fracture Evaluation using reflected Stoneley-wave arrivals. Geophysics, 54, 1274-1288.

Keys, W.A., 1979. Borehole Geophysics in Igneous and Metamorphic Rocks. the 20th Annual Logging Symposium of the SPWLA, Tulsa.

Koerperich, E.A., 1978. Investigation of Acoustic Boundary Waves and Interference Patterns as Techniques for Detecting Fractures. J. Petrol. Techn., 1197–1207.

Kuster, G.T., and Toksoz, M.N., 1974. Velocity Attenuation of Seismic Waves in Two Phase Media: Part 1. Theoretical formulations. Geophysics, 39 (5), 587-606.

Luthi, S.M., and Souhaité, P., 1990. Fracture apertures from electrical borehole scans. Geophysics, 55, 821-833.

Morris, R.L.; Grine, D.A., and Arkfeld, T.E., 1964. Using Compressional and Shear Acoustic Amplitudes. J. Petrol. Techn., 623–632.

Nelson, R.A., 1982. An approach to evaluating fractured reservoirs. J. Petrol. Techn., 2167- 2170.

Norris, A.N., 1989. Stoneley wave attenuation and dispersion in permeable formations. Geophysics, 54, 330-341.

Paillet, F.L., 1991.a. Use of Geophysical Well Logs in Evaluating Crystalline Rocks for Siting of Radioactive Waste Repositories. The Log Analyst, 85–107.

Paillet, F.L., 1991.b. Qualitative and Quantitative Interpretation of Fracture Permeability Using Acoustic Full-Waveform Logs. The Log Analys.,256–270.

Poeter, E.P., 1987. Characterized Fractures at Potential Nuclear Waste Repository Sites with Acoustic Waveform Logs. The Log Analyst, 453–461.

Sibbit, A.M., and Faivre, O., 1985. The Dual Laterolog Response in Fractured Rocks. The 26th Annual Logging Symposium of the SPWLA, Dallas, USA.

Winkler, K.W.; Liu, H.L., and Johnson, D.L., 1989. Permeability and borehole Stoneley waves: comparison between theory and experiment. Geophysics, 54, 66-75

تحليل قياسات الابار لتقدير المسامية في مكامن القاعدة المهشمة

محمود إبراهيم عبدالرازق

لقد امكن وصف المكامن المهشمة منخفضة المسامية وذلك باستخدام المعلومات الهندسية المبينة التفاصيل بدرجة دقة عالية والناتجة من الصور البئرية بالإضافة الى طرق التقييم باستخدام نتائج التسجيلات الاكثر اختراقا.
تم ذلك بالاستعانة بالوسائل الكهربية والصوتية (السيزمية) والتي تعطى التوزيع الاحصائي للكسور – حيث تعبر بدرجة اولى عن الفتحات الناتجة عن الكسور والمسامية فضلا عن المؤشرات الجيولوجية – الا ان هذه الصور تتأثر سلبيا كثيرا بسبب عمليات الحفر.
الطرق الاكثر اختراقا , ولكن ذات الدقة الاقل مثل موجات ستونلي المنعكسة والتسجيل الكهربي المستخدم في تمييز الكسور العميقة المنفذة والمرتبطة بمعدل التدفق للسوائل .
بجعل بعض الفرضيات حول طبيعة المسامية في خزانات صخور القاعدة والصخور المتحولة, لتحديد المسامية والمبنى على نموذج كستر- توكسوز للتشتت والذى يتطلب قياسات ذات تردد منخفض لكل كم الموجات التضاغطية وموجات القص.
وتم تحديد نسبة الطول الى العرض. حيث ظهر ان نسبة الطول الى العرض في الصخور النارية المهشمة تتراوح من ٠,٠١: ٠,٠٠١ , بينما كانت في البريشيا قريبة من ٠,١.